Original Article

Asymmetry assessment using cone beam CT
A Class I and Class II patient comparison

Matthew M. Sievers[a]; Brent E. Larson[b]; Philippe R. Gaillard[c]; Andrew Wey[d]

ABSTRACT

Objective: To estimate possible differences in skeletal asymmetry between patients with skeletal Class I and skeletal Class II relationships.

Materials and Methods: Cone beam computed tomography (CBCT) images were examined from 70 consecutive patients who presented for orthodontic care and fit the inclusion criteria. Asymmetry was quantified using an asymmetry index developed by Katsumata et al. Anatomic landmarks were defined and reference planes were established to determine the asymmetry of the landmarks using a constructed coordinate plane system. Thirty randomly selected patients were reanalyzed to assess the reliability of the method.

Results: Statistical analysis did not find any significant relationship between asymmetry and A-P skeletal relationship for any of the landmarks. Asymmetry index scores were reproducible within a certain range of agreement for each landmark.

Conclusions: Based on this study, the discrepant jaw growth resulting in a Class II skeletal pattern results in no more skeletal asymmetry than Class I skeletal patterns. (*Angle Orthod.* 2012;82:410–417.)

KEY WORDS: Asymmetry assessment; Cone-beam; CBCT; 3 dimensional analysis; Facial asymmetry

INTRODUCTION

Assessing symmetry is important in any esthetic evaluation of the craniofacial region. A previous study by Katsumata et al.[1] described a system for investigating skeletal asymmetry on three-dimensional head radiographs using a skeletal landmark-based system. Such a system could allow accurate comparison of a given orthodontic patient to normative values, and make asymmetry diagnosis more objective.

There are many articles that posit a relationship between malocclusion and cranial skeletal asymmetry. One relationship frequently cited in the literature is the Class II subdivision patient. Janson et al.[2] found that a Class II subdivision patient has the maxillary midline on with the face and the mandibular midline off toward the Class II side 61% of the time, the mandibular midline on with the face and the maxillary midline off 18% of the time, and a combination is present 20% of the time. Alavi et al.[3] examined Class II subdivision patients and primarily found asymmetry in the mandible of these patients.

Another relationship that has been previously investigated is the relationship between ANB angle and facial or skeletal asymmetry. A study by Good et al.[4] divided patients by ANB angle with groups of less than 3 degrees, 3–4 degrees, and greater than 4 degrees, and examined facial photographs for mandibular asymmetry. They found significantly more asymmetry in the less than 3 degrees ANB angle group. A retrospective study by Severt et al.[5] looked at 1460 orthognathic cases treated at the University of North Carolina and found an increased percentage of chin deviation of at least 2 mm from the midline in Class III patients. The purpose of this study is to compare the skeletal symmetry of orthodontic patients

[a] Private Practice, Cambridge, Owatonna, and Faribault, Minn.

[b] Associate Professor and Director, Division of Orthodontics, School of Dentistry, University of Minnesota, Minneapolis, Minn.

[c] Research Assistant, Biostatistical Design and Analysis Center, Clinical and Translational Science Institute, University of Minnesota, Minneapolis, Minn.

[d] Research Associate, Biostatistical Design and Analysis Center, Clinical and Translational Science Institute, University of Minnesota, Minneapolis, Minn.

Corresponding author: Dr Matthew M. Sievers, Cambridge Orthodontics, 140 Birch St N #106, Cambridge, MN 55008 (e-mail: sievers.matthew@gmail.com)

Accepted: August 2011. Submitted: April 2011.
Published Online: October 6, 2011

who have a high ANB angle to those with average ANB angles using CBCT images. The hypothesis is that patients with a skeletal Class II growth pattern, which is a readily identifiable skeletal variation, may also have increased levels of skeletal asymmetry.

Three-dimensional cone beam computed tomography (CBCT) images are uniquely suited to assess asymmetry. These images use a built-in reconstruction algorithm to correct known distortions due to projection geometry,[6] and allow clinicians to assess skull anatomy either through three-dimensional surface renderings or through accurate two-dimensional slices through the skull. Previous methods of asymmetry assessment relied on two-dimensional radiographs with inherent problems not present in CBCT images. Two-dimensional images have variations in magnification with areas closer to the film magnified less than those nearer to the radiation source.[7] Cook[8] found that a posteroanterior cephalometric radiograph with patient head rotation of 5 degrees can cause the apparent side of an asymmetry to switch. Lateral cephalometric radiographic asymmetry studies can be affected by asymmetric external auditory meati locations, which would lead to head rotation and erroneous results. A potential drawback to asymmetry assessment using CBCT images is a lack of a database of symmetric patients as a basis for comparison and asymmetry diagnosis. Such a database would be difficult to create because of concerns about unnecessary radiation exposure of people who may not require a CBCT scan.

There are unique difficulties and advantages associated with identifying craniometric landmarks on three-dimensional CBCT images. Some landmarks can be easily identified in one or two planes of space, but identification in the third plane of space can be difficult. In these cases observers tend to locate the landmarks in the planes of easiest visualization.[9,10] Difficulty is created by inclusion of the medio-lateral dimension to landmark location, a dimension which was not considered when lateral cephalometric landmarks were created.[10] A benefit of CBCT landmark identification is a lack of superimposed structures, which creates easier visualization of certain skull regions. Also, CBCT images are not plagued by geometric distortion.[11–13] Another advantage to CBCT landmark identification is visualization using the stacks of CBCT slices, known as the multiplanar reconstruction (MPR) images. This allows inspection from any of the three planes of space to help identify landmarks from multiple views. Grauer et al.[14] recommends identifying landmarks on the MPR images rather than on the three-dimensional surface rendering as the rendered image is dependent on factors such as image contrast, movement during acquisition, signal-to-noise ratio of the image, and threshold filters applied by the operator.

There are several variables that could influence accuracy of linear measurements reported in the literature. Voxel size, type of image detector, scanning time, reconstruction time, radiation dose, and head position have been mentioned as variables that could affect CBCT linear measurements.[9,15] Two previous studies have investigated the effect of head position on linear measurements and found it insignificant.[16,17] Another study compared measurement accuracy using two different voxel settings with no difference in accuracy between the two groups.[17] Overall, various studies have investigated the accuracy of landmark localization on CBCT images. Many have found the process both accurate and reproducible[10,17–19] Other studies have investigated linear measurements using CBCT images and support the accuracy of such measures.[15,20–25]

MATERIALS AND METHODS

This study was reviewed and approved by the Ethics Committee at the University of Minnesota. This study examined CBCT images of 70 patients presenting for routine orthodontic treatment at the University of Minnesota obtained as part of diagnostic record gathering. The use of CBCT was not based on any clinical assessment of asymmetry. IRB approval was obtained to review these CBCT images. ANB angles were measured on simulated lateral cephalometric images extracted from the CBCT radiographs and digitized using Dolphin 11.5 betabuild 15 (Dolphin Imaging and Management Solutions, Chatsworth, Calif). The Class I group consisted of 30 patients with ANB angles ranging from −0.5 degrees to 3.4 degrees. The Class II group consisted of 30 patients with ANB angles of 4.5 and higher. A third group of 10 patients was included that had ANB angles between 3.4 and 4.4 degrees to enable the examination of ANB as a continuous variable. The inclusion criteria were patients age 11 years 0 months to age 15 years 11 months with CBCT films who fit into a required ANB group angle. Patients were excluded if they had been identified during clinical examination, or through examination of the photographs, to have a CR/CO shift, a posterior crossbite, a first molar in dental crossbite, a lack of a first molar, or a craniofacial anomaly or syndrome including cleft lip or cleft palate. The patients were consecutively selected starting from July 2008 until the required patient groups were filled.

CBCT images were acquired with a Next Generation iCAT CBCT unit (Imaging Sciences International, Hatfield, Penn). The device was set for 18.54 mAs and 120 kV. The scan was made with a single

Table 1. Landmark Definitions for Asymmetry Assessment

Landmark		Definition on CBCT Image
Landmarks for the determination of the reference planes	Sella	Center of the pituitary fossa
	Nasion	Nasofrontal suture at the midline
	Dent	The most superior point of the dens on the axis
Landmarks for the evaluation of facial asymmetry (* denotes bilateral landmarks)	ANS	Tip of the anterior nasal spine
	Upper Central Incisors (UCI)	The crest of the alveolar ridge between the upper central incisors
	Lower Central Incisors (LCI)	The crest of the alveolar ridge between the lower central incisors
	Menton	The lower border of the mid-mandibular suture
	Orbitale*	The mid-point of the infra-orbital margin
	Porion*	The superior surface of the external auditory meatus
	Upper First Molar (UFM)*	The center of the pulp cavity at the crown of the upper first molar
	Lower First Molar (LFM)*	The center of the pulp cavity at the crown of the lower first molar
	Condyle *	The most superior point of the condyle
	Coronoid*	The most superior point of the coronoid process
	Gonion*	The most inferior and posterior point at the angle of the mandible

360-degree rotation, 8.9-second scan with a voxel size of 0.3 mm. The head was oriented with the midsagittal plane perpendicular to the floor. Patients were biting in centric occlusion during exposure. DICOM files obtained from the CBCT scan were reconstructed by Dolphin 3D, which is part of Dolphin 11.5 (betabuild 15); all landmark identifications and measurements were made using this software. Images were visualized on a Dell 1908FP monitor (Dell Inc, Round Rock, Tex) with a resolution of 1280 X 1024 at 60 Hz.

Asymmetry assessment for this study was conducted in a manner similar to a study by Katsumata et al.[1] Craniometric landmarks were identified as defined in Table 1. Figure 1 demonstrates the MPR slices and three-dimensional reconstructions used to locate each landmark. All landmarks in this study were identified by the primary author. This study strove to use whichever views were most advantageous for localizing each landmark. The views varied from landmark to landmark, but were constant between subjects. For most landmarks, identification was limited to MPR images only. In identifying orbitale, the three-dimensional surface rendering was used as it allowed better medio-lateral localization. In identifying gonion, the three-dimensional surface rendering was used as it gave a broad picture of the ramus and body, making anterior-posterior and superior-inferior identification more accurate. This study did not include the landmark pterygomaxillary fissure as included by Katsumata et al.[1] as preliminary investigation demonstrated difficulty in accurate identification.

The landmarks Sella, Nasion, and Dent were used to create the three reference planes used to measure linear landmark distances (Figure 2). The mid-saggital plane was defined as passing through the landmarks Sella, Nasion, and Dent. The axial plane was defined as passing through Sella and Nasion and being perpendicular to the mid-saggital plane. The coronal plane was defined as being perpendicular to the other two planes and passing through Dent. For the remaining landmarks, the distance to each plane was calculated by Dolphin 3D in millimeters by orienting the coordinate plane system to the reference planes. This gave a dx, dy, and dz value for that landmark, with dx the distance to the saggital plane, dy the distance to the axial plane, and dz the distance to the coronal plane.

For solitary landmarks located near the midline, the asymmetry indices (AI) were defined as the distance to the sagittal plane (AI = dx). For bilateral landmarks the asymmetry indices were calculated using the following formula, where R = right, L = left:

$$AI = \sqrt{(Rdx - Ldx)^2 + (Rdy - Ldy)^2 + (Rdz - Ldz)^2}$$

Thirty patients were randomly selected using a random number generator to have landmarks and reference planes re-identified and asymmetry indexes recalculated two weeks later to test the intra-examiner reliability of the presented method.

RESULTS

The Class I group had a mean ANB angle of 1.7 degrees (SD 1.2, range −0.5 to 3.4). The mean age was 13 years 3 months (SD 1y 1mo, range 11y 2mo to 15y 1mo). The Class II group had a mean ANB angle of 6.3 degrees (SD 1.4, range 4.6 to 10.2). The mean age for this group was 13 years 3 months (SD 1y 3mo, range 11y 5mo to 15y 11mo). The group of 10 patients had a mean ANB angle of 4.0 degrees (SD 0.3, range 3.5 to 4.4). The mean age for this group was 13 years 4 months (SD 1y 1mo, range 11y 9mo to 15y 1mo).

Pearson correlation coefficients measuring the linear relationship of ANB to asymmetry index score were calculated for each landmark across all patients

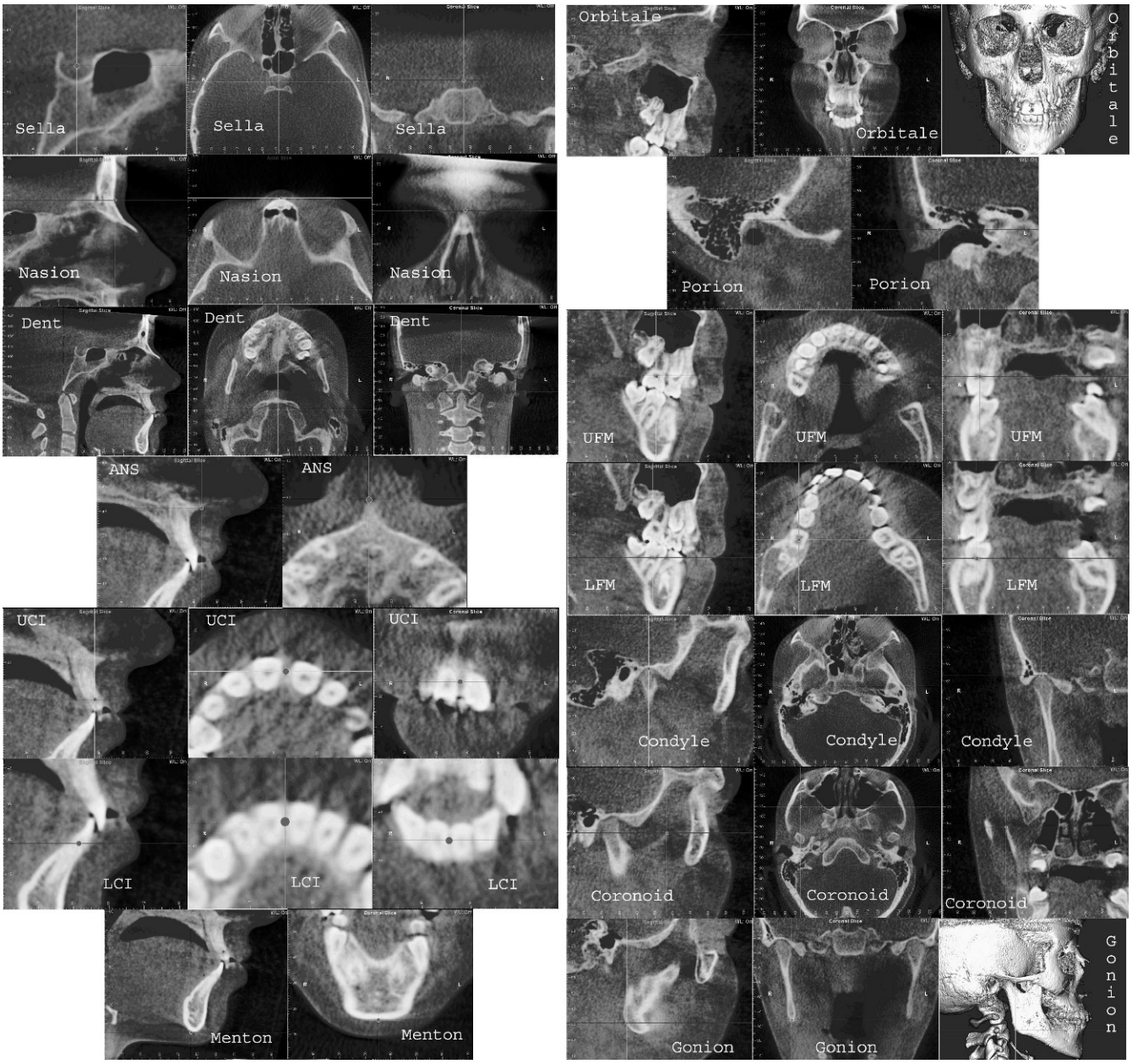

Figure 1. MPR slices and three-dimensional reconstructions used to locate each landmark.

and the results are presented in Table 2. None of the coefficients are statistically significant for a linear relationship between ANB and asymmetry index score for any landmark. Visual inspection of scatter plots gives no apparent support for any non-linear relationships between ANB and asymmetry index score.

ANOVA results compared mean asymmetry index scores between Class I and Class II ANB angle groups of patients. Table 3 gives F and *P* values for each ANOVA test for each landmark. No significant differences in the mean asymmetry index values were found for any landmark.

Because there were no significant differences in asymmetry index scores relative to ANB angle, the scores from all groups were combined to find an asymmetry index mean score and standard deviation for each landmark (Table 4). Reproducibility of asymmetry index scores was assessed through repeat measurement of 30 randomly selected patients. Altman-Bland plots[26] compared original and repeated measurement data for each landmark as well as for dx, dy, and dz. Table 5 presents a summary of the Altman-Bland plots. The data does not demonstrate average bias for any landmark.

Figure 2. The reference planes used in this study demonstrated on MPR images and three-dimensional reconstruction.

DISCUSSION

This study used a previously developed three-dimensional asymmetry analysis system to investigate the relationship between skeletal Class II patients and asymmetry. The results of this study do not support a relationship between increasingly positive ANB angles and skeletal asymmetry. The data does not approach significance for any craniometric landmark. A future research study could investigate three-dimensional asymmetry among groups of patients known to be asymmetric, such as Class II subdivision patients or unilateral posterior crossbite patients, to test the sensitivity of this method. It is noted that the range of agreement for each landmark limits this index's ability to diagnose asymmetry on an individual patient. It may be best utilized as it was in this study, for comparing large groups and testing asymmetry differences for a specific trait.

Table 2. Pearson Correlation Coefficients of ANB and Asymmetry Index Score Across All Patients

Landmark	Correlation Coefficient	*P* Value
ANS	.110	.365
Upper Central Incisors	.139	.252
Lower Central Incisors	.105	.387
Menton	.078	.522
Orbitale	−.078	.520
Porion	.072	.551
Upper First Molar	.085	.483
Lower First Molar	.143	.236
Condyle	−.011	.927
Coronoid	.060	.619
Gonion	.054	.660

Katsumata et al.[1] used the mean asymmetry index scores and standard deviations to establish ranges for symmetry, asymmetry, and marked asymmetry for a particular landmark. Their baseline for calling a

Table 3. ANOVA Analysis of the Relationship Between Angle Classification and Asymmetry Index

Landmark	Class	Mean AI	F Value	*P* Value
ANS	Class 1	1.43	1.89	.174
	Class 2	1.91		
Upper Central Incisors	Class 1	1.93	2.07	.156
	Class 2	2.56		
Lower Central Incisors	Class 1	2.39	1.31	.257
	Class 2	2.92		
Menton	Class 1	3.37	.62	.433
	Class 2	3.85		
Orbitale	Class 1	4.22	.01	.932
	Class 2	4.26		
Porion	Class 1	3.97	.79	.379
	Class 2	4.52		
Upper First Molar	Class 1	4.05	1.35	.251
	Class 2	4.90		
Lower First Molar	Class 1	4.97	2.15	.148
	Class 2	6.13		
Condyle	Class 1	4.24	.05	.829
	Class 2	4.36		
Coronoid	Class 1	3.90	1.24	.270
	Class 2	4.52		
Gonion	Class 1	5.41	1.09	.300
	Class 2	6.31		

landmark asymmetric was the mean for the landmark plus one standard deviation. They defined a landmark as markedly asymmetric if its asymmetry index score was twice the baseline level for asymmetry. Figure 3 demonstrates graphically the boundaries for asymmetry and marked asymmetry diagnosis using the method of Katsumata et al.,[1] as well as the new boundaries for diagnosis if means and standard deviations from the present study are used. The boundaries are higher in the present study as Katsumata's study utilized patients who were selected for lack of asymmetry. Using either set of norm values it may be more advantageous to report the number of standard deviations from the mean rather than specific cutoffs for asymmetry and marked asymmetry which can oversimplify the information provided from the index. Future studies of known asymmetric populations using CBCT may clarify recommended values for asymmetry diagnosis using this index.

Table 4. Asymmetry Index Means ± SD with All Patients Combined

Landmark	Asymmetry Index Mean ± SD
ANS	1.6 ± 1.3
Upper Central Incisors	2.2 ± 1.7
Lower Central Incisors	2.6 ± 1.7
Menton	3.5 ± 2.3
Orbitale	4.2 ± 1.6
Porion	4.2 ± 2.3
Upper First Molar	4.3 ± 2.8
Lower First Molar	4.3 ± 2.0
Condyle	5.4 ± 3.0
Coronoid	4.2 ± 2.4
Gonion	5.7 ± 3.2

Table 5. Altman-Bland Analysis with Bias and 95% CI

Landmark	Bias (95% CI)
ANS	−.007 (−1.866, 1.852)
Upper Central Incisor	−.013 (−2.065, 2.039)
Lower Central Incisor	.030 (−2.308, 2.368)
Menton	−.187 (−3.198, 2.824)
Orbitale	.423 (−3.015, 3.861)
Porion	−.239 (−3.009, 2.531)
Upper First Molar	−.049 (−3.097, 2.999)
Condyle	.005 (−2.623, 2.633)
Lower First Molar	.136 (−3.528, 3.800)
Coronoid	−.423 (−3.462, 2.616)
Gonion	.235 (−4.064, 4.534)
dx	.169 (−2.512, 2.849)
dy	−.115 (−2.132, 1.903)
dz	−.050 (−1.868, 1.767)

Landmark identification errors are likely the main source of error in this study. Altman Bland analysis indicated that for this study reproducibility was poorest in the mediolateral dimension (dx). There are extra difficulties in identifying landmarks on living human scans which can lead to errors, such as reductions in image quality due to soft-tissue attenuation, metallic artifacts, and patient motion.[15] Creating the three reference planes requires identifying the landmarks sella, nasion, and dent. Each of these landmarks requires identifying a centroid of a specific three-dimensional structure and thus qualifies as a "fuzzy landmarks."[17,18] Any identification error of these landmarks leads to a built-in error for all asymmetry index measures. Even the relatively easy to identify landmark ANS has a range of 95% agreement for the asymmetry index of nearly two units in either direction. It is possible that this range of agreement for ANS asymmetry index scores is mostly due to variability in landmark identification of the reference landmarks and consequently variability in the reference planes. Ideally, a system of reference planes would be based upon easy to identify anatomic landmarks which should increase the accuracy and reliability of this system.

Orienting the reference planes using Dolphin 3D created another source of error. The reference planes had to be manually oriented to pass through the center of each of the required reference landmarks. Dolphin 3D is able to identify how far the reference planes are located from the center of each of the landmarks, and this error was minimized by not allowing the reference planes to pass greater than 0.2 mm away from the center of the landmarks before accepting the plane locations.

Dolphin 3D automatically calculated the linear distances from each landmark to each of the reference planes in millimeters. Because the linear measurement portion of the analysis was automated, it is not a likely source of further error in this study.

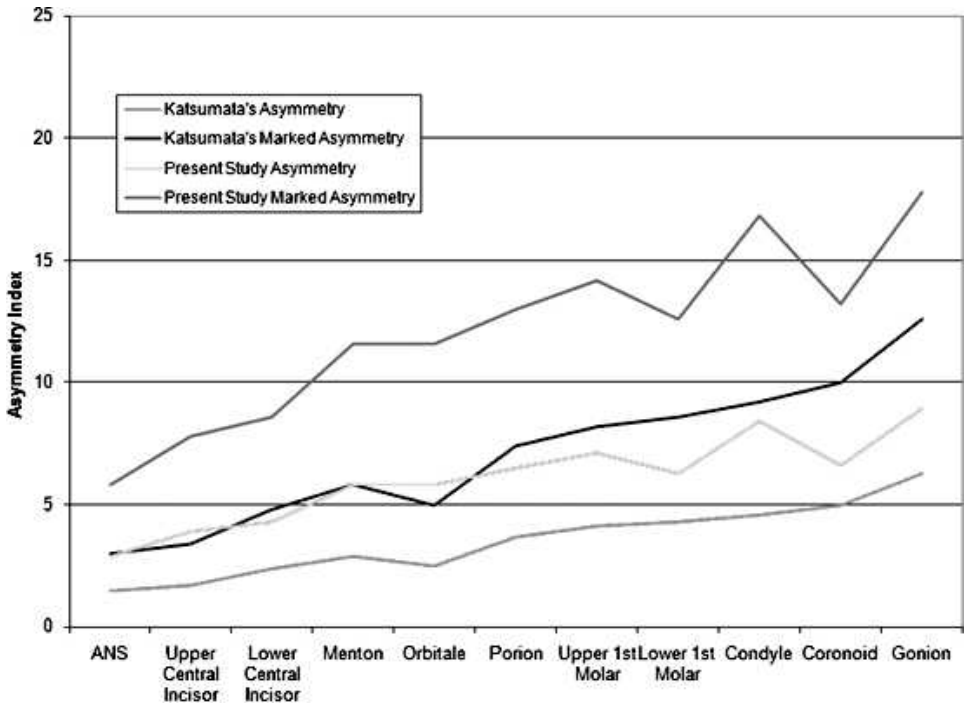

Figure 3. Katsumata et al.[1] asymmetry diagnosis boundaries compared to asymmetry diagnosis boundaries using the means and standard deviations from the current study.

CONCLUSION

- Based on this study, the discrepant jaw growth resulting in a Class II skeletal pattern results in no more skeletal asymmetry than Class I skeletal patterns.

ACKNOWLEDGMENT

This article is based on a master's thesis by the primary author available in its entirety at: http://conservancy.umn.edu/bitstream/93384/1/Sievers_Matthew_June2010.pdf

REFERENCES

1. Katsumata A, Fujishita M, Maeda M, Ariji Y, Ariji E, Langlais RP. 3D-CT evaluation of facial asymmetry. *Oral Surg Oral Med Oral Pathol Oral Radiol Endod*. 2005;99:212–220.
2. Janson G, de Lima KJ, Woodside DG, Metaxas A, de Freitas MR, Henriques JF. Class II subdivision malocclusion types and evaluation of their asymmetries. *Am J Orthod Dentofacial Orthop*. 2007;131:57–66.
3. Alavi DG, BeGole EA, Schneider BJ. Facial and dental arch asymmetries in class II subdivision malocclusion. *Am J Orthod Dentofacial Orthop*. 1988;93:38–46.
4. Good S, Edler R, Wertheim D, Greenhill D. A computerized photographic assessment of the relationship between skeletal discrepancy and mandibular outline asymmetry. *Eur J Orthod*. 2006;28:97–102.
5. Severt TR, Proffit WR. The prevalence of facial asymmetry in the dentofacial deformities population at the University of North Carolina. *Int J Adult Orthodon Orthognath Surg*. 1997;12:171–176.
6. Carlson CA. Imaging modalities in x-ray computerized tomography and in selected volume tomography. *Phys Med Biol*. 1999;44:R23–56.
7. Terajima M, Nakasima A, Aoki Y, et al. A 3-dimensional method for analyzing the morphology of patients with maxillofacial deformities. *Am J Orthod Dentofacial Orthop*. 2009;136:857–867.
8. Cook JT. Asymmetry of the cranio-facial skeleton. *Br J Orthod*. 1980;7:33–38.
9. de Oliveira AE, Cevidanes LH, Phillips C, Motta A, Burke B, Tyndall D. Observer reliability of three-dimensional cephalometric landmark identification on cone-beam computerized tomography. *Oral Surg Oral Med Oral Pathol Oral Radiol Endod*. 2009;107:256–265.
10. Ludlow JB, Gubler M, Cevidanes L, Mol A. Precision of cephalometric landmark identification: Cone-beam computed tomography vs conventional cephalometric views. *Am J Orthod Dentofacial Orthop*. 2009;136:312.e1–10; discussion 312–313.
11. Brodie AG. Cephalometric roentgenology; history, technics and uses. *J Oral Surg (Chic)*. 1949;7:185–198.
12. Chien PC, Parks ET, Eraso F, Hartsfield JK, Roberts WE, Ofner S. Comparison of reliability in anatomical landmark identification using two-dimensional digital cephalometrics and three-dimensional cone beam computed tomography in vivo. *Dentomaxillofac Radiol*. 2009;38:262–273.
13. Salzmann JA. Limitations of roentgenographic cephalometrics. *Am J Orthod*. 1964;50:169–188.
14. Grauer D, Cevidanes LS, Proffit WR. Working with DICOM craniofacial images. *Am J Orthod Dentofacial Orthop*. 2009;136:460–470.
15. Periago DR, Scarfe WC, Moshiri M, Scheetz JP, Silveira AM, Farman AG. Linear accuracy and reliability of cone beam CT derived 3-dimensional images constructed using an orthodontic volumetric rendering program. *Angle Orthod*. 2008;78:387–395.
16. Damstra J, Fourie Z, Huddleston Slater JJ, Ren Y. Accuracy of linear measurements from cone-beam computed tomography-derived surface models of different voxel sizes. *Am J Orthod Dentofacial Orthop*. 2010;137:16.e1–6; discussion 16–17.

17. Kragskov J, Bosch C, Gyldensted C, Sindet-Pedersen S. Comparison of the reliability of craniofacial anatomic landmarks based on cephalometric radiographs and three-dimensional CT scans. *Cleft Palate Craniofac J*. 1997;34: 111–116.
18. Valeri CJ, Cole TM III, Lele S Richtsmeier JT. Capturing data from three-dimensional surfaces using fuzzy landmarks. *Am J Phys Anthropol*. 1998;107:113–124.
19. Komori M, Kawamura S, Ishihara S. Averageness or symmetry: Which is more important for facial attractiveness? *Acta Psychol (Amst)*. 2009;131:136–142.
20. Berco M, Rigali PH Jr, Miner RM, DeLuca S, Anderson NK, Will LA. Accuracy and reliability of linear cephalometric measurements from cone-beam computed tomography scans of a dry human skull. *Am J Orthod Dentofacial Orthop*. 2009;136:17.e1–9; discussion 17–18.
21. Hilgers ML, Scarfe WC, Scheetz JP, Farman AG. Accuracy of linear temporomandibular joint measurements with cone beam computed tomography and digital cephalometric radiography. *Am J Orthod Dentofacial Orthop*. 2005;128: 803–811.
22. Ludlow JB, Laster WS, See M, Bailey LJ, Hershey HG. Accuracy of measurements of mandibular anatomy in cone beam computed tomography images. *Oral Surg Oral Med Oral Pathol Oral Radiol Endod*. 2007;103:534–542.
23. Pinsky HM, Dyda S, Pinsky RW, Misch KA, Sarment DP. Accuracy of three-dimensional measurements using cone-beam CT. *Dentomaxillofac Radiol*. 2006;35:410–416.
24. Richtsmeier JT, Paik CH, Elfert PC, Cole TM III, Dahlman HR. Precision, repeatability, and validation of the localization of cranial landmarks using computed tomography scans. *Cleft Palate Craniofac J*. 1995;32:217–227.
25. Williams FL, Richtsmeier JT. Comparison of mandibular landmarks from computed tomography and 3D digitizer data. *Clin Anat*. 2003;16:494–500.
26. Bland JM, Altman DG. Statistical methods for assessing agreement between two methods of clinical measurement. *Lancet*. 1986:307–310.